

Performance Evaluation of the IEEE 802.11a and b WLAN Physical Layer on the Martian Surface

Deva K. Borah, Anirudh Daga, Gaylon R. Lovelace and Phillip De Leon

New Mexico State University

Klipsch School of Electrical and Computer Engineering

Las Cruces, NM 88003

(505) 646-3357

{dborah, anirudh, glovelac, pdeleon}@nmsu.edu

Abstract—The performance of IEEE 802.11a and b WLAN standards on the Martian surface is studied. The Gusev Crater region and the Meridiani Planum (Hematite) region are chosen as example sites based on the mission science and mission success criteria. The radio frequency (RF) multipath environment is obtained using digital elevation maps (DEMs) from the Mars Global Surveyor mission, taking into account the atmosphere and other factors on the Martian surface. It is observed that IEEE 802.11a performs well in terms of packet error rates at distances up to a few hundred meters from the transmit antenna when the transmit power is 1 W and the antennas are located 1.5 m above the ground. Although the performance of IEEE 802.11b is found to be more adversely affected, its performance too can be improved significantly using a RAKE receiver. It is observed that the lower data rate modes of 802.11a show much better results in terms of bit error rates. However, both 802.11a and b appear to provide effective communications within a few hundred meters of the transmitter in the selected sites considered.

TABLE OF CONTENTS

- 1 INTRODUCTION**
- 2 IEEE 802.11 WLAN**
- 3 RF ENVIRONMENT ON THE MARTIAN SURFACE**
- 4 PERFORMANCE AT DIFFERENT SITES**
- 5 DISCUSSION**
- 6 CONCLUSIONS**

1. INTRODUCTION

Future space missions on the Martian surface may involve multiple rovers collecting data at different locations, and communicating wirelessly with common access points. Such communications have to be reliable, robust and power efficient. Development and testing of such communication technologies from scratch is an expensive proposition. A more cost effective approach would be to adapt existing technology with appropriate modifications. Towards this objective,

this paper investigates the physical layer performance of two well known wireless local area network (WLAN) standards IEEE 802.11a and IEEE802.11b under the Martian environment, and identifies the issues that need to be addressed.

The IEEE 802.11b standard [1] provides data rate options of 1, 2, 5.5 and 11 Mbit/s in the 2.4 GHz band. The modulation options include direct sequence spread spectrum using differential binary phase shift keying (BPSK), quadrature phase shift keying (QPSK), complementary code keying (CCK), and packet binary convolutional code (PBCC). Although primarily designed for indoor office environments, recent studies have shown good performance of 802.11b in outdoor environments [2], [3]. However, the performance with low height rover antennas on the Martian surface, and the performance comparison of 802.11b with respect to 802.11a in the Martian environment are important issues that have not been addressed before and need investigation.

The IEEE 802.11a standard [4] operates in the 5 GHz band and uses the orthogonal frequency division multiplexing (OFDM) technology. It can support data rates of 6, 9, 12, 18, 24, 36, 48, and 54 Mbit/s. The standard employs convolutional encoder, and uses cyclic prefix of 0.8 micro second duration. This enables it to handle the multipath problem more successfully [5], [6]. However, longer delay spreads, that can happen on the Martian environment with low height antennas and longer transmitter/receiver distances, can severely affect its performance. Therefore, the effects of such delay spreads on the Martian surface require investigation.

In previous work [7], the RF environment of the Martian surface has been extensively studied. In particular, the RF coverage patterns produced from a 2.4 GHz transmitter with 1 W radiated power and 1 m antenna height within Gusev Crater and Meridiani Planum have been investigated. These simulations use 11 m/pixel digital elevation maps from the Mars Global Surveyor mission. The software used in this study takes into account the propagation factors such as planetary radius, atmospheric density and composition, soil chemistry, etc. The impact of surface clutter (rocks) on RF propagation has also been examined. It has been observed in that study that while significant terrain variation can have a major impact on the coverage, sufficient RF signal power for an IEEE

This work was supported by NASA Grant NAG3-2864
0-7803-8870-4/05/\$20.00 ©2005 IEEE
IEEEAC paper #1237, Version 2, Dec. 10, 2004

802.11b link is possible at these sites over several kilometer distances even with low antenna heights.

This paper uses the received power results from [7] and recent results regarding the simulation of the multipath environment in the performance evaluation of the 802.11 a and b standards. We study the performance of different data rates for different transmit and receive antenna locations and several sites on Mars. It is observed that multipaths can severely affect the performance of 802.11b. The use of receivers that take care of multipaths (such as RAKE) is found to provide significant improvement. The performance of 802.11a is also found to be affected by the multipath environment, especially in the absence of clear line-of-sight. In particular, the higher bit rate modes of IEEE 802.11a are found to be more affected by the multipaths. Further, when the delay spread exceeds the $0.8 \mu\text{s}$ cyclic prefix duration, the performance drops rapidly.

This paper is organized as follows. In Section 2, we provide an overview of the 802.11a and b physical layer (PHY) specifications. The packet structures described in this section are faithfully simulated in our simulation results section. In Section 3, the site selection criteria on the Martian surface, and the radio frequency (RF) multipath calculation are described. Section 4 presents the simulation results in terms of packet error rates and bit error rates. A discussion on the interpretations of the simulation results is presented in Section 5. Finally, Section 6 presents the conclusions of our study.

2. IEEE 802.11 WLAN

In this section, we present a brief overview of the physical layer specifications of IEEE 802.11a and b standards.

IEEE 802.11a

The IEEE 802.11a PHY is based on orthogonal frequency division multiplexing (OFDM) and operates in the 5 GHz band providing data payload capabilities of 6, 9, 12, 18, 24, 36, 48 and 54 Mbit/s. The different transmission rates are obtained by varying the modulation type and/or the channel coding rates. The system uses 52 subcarriers that are modulated using BPSK, QPSK, 16- or 64-quadrature amplitude modulation (QAM). The error correction coding uses a convolutional encoder with a coding rate of 1/2, 2/3 or 3/4.

The physical layer protocol data unit (PPDU) format is shown in Fig. 1. The physical layer convergence procedure (PLCP) preamble field consists of 10 repetitions of a short training sequence, and two repetitions of a long training sequence preceded by a guard interval (GI). A single BPSK encoded OFDM symbol follows. It contains a 4-bit RATE field, a 12 bit LENGTH field, one reserved bit, one parity bit and 6 ‘zero’ tail bits encoded with a rate 1/2 convolutional code. The DATA portion contains a 16 bit SERVICE field, a physical sublayer service data unit (PSDU), 6 ‘zero’ tail bits and pad bits, and may constitute multiple OFDM symbols.

PLCP Preamble 12 symbols	SIGNAL One OFDM symbol	DATA OFDM symbols
-----------------------------	---------------------------	----------------------

(a) IEEE 802.11a

PLCP Preamble 144 bit or 72 bit	PLCP Header 48 bit	PSDU
------------------------------------	-----------------------	------

(b) IEEE 802.11b

Figure 1. PPDU Format for IEEE 802.11a and b.

The data to be transmitted are scrambled to remove any spectral line from the data. They are then convolutionally encoded with a rate 1/2 encoder with generator polynomials $g_0 = 133_8$, $g_1 = 171_8$, and puncturing is performed if necessary. All encoded data bits are interleaved using two steps. First, consecutive coded bits are mapped to non-adjacent subcarriers. The second step maps consecutive coded bits onto the less and more significant bits of the constellation.

The OFDM symbols are transmitted using a relatively long cyclic prefix of duration $T_{GI} = T_{FFT}/4$, where T_{FFT} is the duration of an OFDM symbol. The duration T_{FFT} equals $3.2 \mu\text{s}$. Thus the symbol interval is $4.0 \mu\text{s}$. The PLCP preamble duration is $16 \mu\text{s}$, and the SIGNAL symbol lasts $4.0 \mu\text{s}$.

IEEE 802.11b

The IEEE 802.11b direct sequence spread spectrum (DSSS) can provide data rates of 1, 2, 5.5 and 11 Mbit/s in the 2.4 GHZ band. The basic data rate of 1 Mbit/s is provided using differential binary phase shift keying (DBPSK) while the 2 Mbit/s rate uses differential quadrature phase shift keying (DQPSK). The above two data rates employ 11 chip long Barker sequences for spreading with a chip rate of 11 MHz.

Higher data rates of 5.5 Mbit/s and 11 Mbit/s are available in 802.11b through the use of complementary code keying (CCK) at the same chipping rate of 11 Mchips/s. Each CCK symbol consists of 8 complex chips: $e^{j(\phi_1+\phi_2+\phi_3+\phi_4)}$, $e^{j(\phi_1+\phi_3+\phi_4)}$, $e^{j(\phi_1+\phi_2+\phi_4)}$, $-e^{j(\phi_1+\phi_4)}$, $e^{j(\phi_1+\phi_2+\phi_3)}$, $e^{j(\phi_1+\phi_3)}$, $-e^{j(\phi_1+\phi_2)}$, $e^{j\phi_1}$. In the case of 5.5 Mbit/s, 4 bits are transmitted per symbol while in the case of 11 Mbit/s, the number of bits transmitted per symbol is 8. The first two bits are used to compute a phase change for ϕ_1 with respect to phase ϕ_1 of the preceding symbol or the phase of the preceding DQPSK symbol if there is a header to PSDU transition. In the case of 5.5 Mbit/s, the remaining two bits are used to derive the phase ϕ_2 , ϕ_3 and ϕ_4 , while the 11 Mbit/s mode uses the remaining 6 bits to compute ϕ_2 , ϕ_3 and ϕ_4 based on QPSK. An optional mode replacing CCK modulation with packet binary convolutional coding (PBCC) with

a 64-state encoder is also available.

The PPDU format for IEEE 802.11b is also shown in Fig. 1. Two different preamble and headers are defined: long PLCP PPDU format and short PLCP PPDU format. The long format contains a 144-bit preamble and a 48-bit header, while the short format contains a 72-bit preamble and a 48-bit header. The preamble contains two fields: synchronization (Sync) and start frame delimiter (SFD). The Sync field is provided to enable the receiver perform necessary synchronization operations. The SFD indicates the start of PHY-dependent parameters within the PLCP preamble. The header consists of signal, service, length and cyclic redundancy code (CRC) fields. The signal field indicates the data rate that is used for the transmission and reception of the PSDU. The service field contains 8 bits, and they carry some information about modulation, symbol clock etc. The length field indicates the number of microseconds required to transmit the PSDU. Finally, a 16 bit CRC protects the signal, service and the length fields. The long PLCP preamble and header are both transmitted using 1 Mbit/s DBPSK modulation. In the case of a short PLCP, the preamble is transmitted using 1 Mbit/s while the header is transmitted using 2 Mbit/s. The transmitted data bits are scrambled at the transmitter and descrambled at the receiver.

3. RF ENVIRONMENT ON THE MARTIAN SURFACE

We have used the ICS Telecom software from ATDI [8] to obtain the multipath environment on the Martian surface. DEM files are converted to ATDI's format for the Martian sites (11m/pixel resolution), and are loaded into the software.

Site Selection

We have selected the Gusev Crater and the Meridiani Planum (Hematite) regions [9] as example sites for our study. These two regions are chosen considering the mission science and mission success criteria [9], [10]. The mission science criteria included evidence of water on the Martian surface in the past. The Gusev Crater appears to have been a lake fed by a river at one time. The Meridiani Planum region shows the chemical signature of Hematite minerals associated with ancient water locations. For mission success, the sites are chosen “near the equator, low in elevation, not too steep, not too rocky, and not too dusty” in addition to other factors. The locations of the selected sites are shown in Table 1.

Table 1. Sites for WLAN Performance Study.

Site	Mars Latitude	Mars Longitude
Gusev1 - Site 1	14° 47' 39.35" S	176° 1' 29.18" E
Gusev1 - Site 2	14° 58' 41.95" S	176° 2' 53.51" E
Gusev1 - Site 3	15° 11' 35.66" S	176° 4' 31.23" E
Hematite4 - Site 1	2° 11' 0.69" S	-5° 53' 5.16" E
Hematite5 - Site 1	1° 52' 29.16" S	-5° 25' 39.59" E

RF Model

The irregular terrain model (ITM) has been used. It is a general-purpose propagation model for frequencies between 20MHz and 20GHz. This model predicts the median attenuation of a radio signal as a function of distance and the variability of the signal in time and space. The predictions are based on electromagnetic theory and statistical analysis of both terrain features and radio measurements.

The ITM source code has been modified for Martian parameters. Atmospheric attenuation is negligible—actual calculations for a horizontal path on Mars' surface yield attenuation of approximately 10^{-6} dB/Km at 2.5GHz [11]. The ITM source code for propagation on Earth accounts for atmospheric refraction by introducing an “effective radius” multiplier of $K = 1.33$. The effective radius used for Earth is K times Earth's physical radius. Mars' atmosphere is so diffuse, even at the planet's surface, as to resemble a vacuum compared to Earth's. Thus we assume atmospheric refraction is negligible in our study [11], [12]. We set $K = 1$, and use an effective radius equal to Mars' physical radius. We note that in some implementations, an effective curvature (inverse of the effective radius) is used.

4. PERFORMANCE AT DIFFERENT SITES

Data packets for 802.11a or 802.11b are generated according to the PPDU format shown in Fig. 1. The simulation software is developed around the mWLAN toolbox from CommAccess Technologies [13]. The data packets from the transmitter are sent through a random multipath channel generated for the particular transmitter and receiver locations on the Martian surface using the ICS Telecom software. The received packets are processed by the corresponding receiver. The 802.11b receiver's performance is studied with and without a RAKE structure. Note that a RAKE receiver coherently combines different multipath contributions before detection and thus improves performance. For both 802.11a and b, only truncated channel impulse responses are estimated at the receiver using the corresponding PLCP Preamble.

Performance versus distance between the transmitter and the receiver

In order to obtain packet error rate (PER) and bit error rate (BER) results versus distance, it is necessary to estimate both the received signal and the input-referred noise for an 802.11 receiver on the Martian surface. The RF propagation simulations using ICS Telecom provide an estimate of electric field intensity at the receiving antenna. A first-order estimate of receiver noise is based on a noise figure $F_R = 7.2$ dB for a typical 802.11a receiver implementation [14]. Assuming noise figure is measured for a reference temperature $T_0 = 290$ K, the equivalent noise temperature for the Martian receiver may be calculated [15] as $T_R = (F_R - 1)T_0 = 1522$ K. An omnidirectional antenna pattern sees roughly half sky and half surface, so we approximate the brightness temperature (T_b) as $T_b = T_p/2 = 250$ K / 2, where T_p is the

physical temperature. Further assuming a radiation efficiency $\eta = 0.9$, we find an equivalent temperature for the antenna of $T_A = \eta T_b + (1 - \eta)T_p = 138$ K. Thus, our simulations use an equivalent noise temperature for the receiver input of $T_{eq} = T_A + T_R = 1560$ K.

The packet error rates (PER) for various distances (d) between the transmitter and receiver are given in Tables 2–6. Note that a CRC failure is considered as a packet error in 802.11b while any error in the OFDM SIGNAL symbol constitutes a packet error in 802.11a. Transmit power is 1 W, and antenna height is 1.5 m above the ground, for both 802.11a and b. The 802.11b results in the table are obtained without RAKE. The data rates for 802.11a and b are 12 Mbps and 11 Mbps respectively.

The packet error rate tables show that both 802.11a and b perform well for receivers within several hundred meters from the transmitter. In some cases, we find better packet error performance at a longer distance (d). For example, with 802.11a at Gusev1 Site2, PER at 500 m appears to be better than the PER at 200 m. Similarly, in the case of Hematite4 Site1, the PER at 200 m is better than the PER at 100 m. In the case of Gusev1 Site2, we observe that while the received power is higher at 200 m, the rms delay spread in this case is smaller for $d = 500$ m, resulting in fewer packet errors. A similar comment can be made about the Hematite4 Site1 PER result. In the case of 802.11b, the performance at 100 m is better than the performance at 50 m for Gusev1 Site2 as well as for Hematite4 Site1. We notice a similar phenomenon as observed in the case of 802.11a, that is, although the received power is smaller for 100 m, the rms delay spread becomes smaller too. Thus, it appears that when sufficient power is transmitted (1 W in this case) the multipath effects play a dominant role on the performance of both 802.11a and 802.11b. Finally, we note that the results with very low PER values must be used with caution as they are not statistically significant due to the small number of packet errors observed from transmitting 20,000 data packets.

The effect of distance on the bit error rate (BER) performance is shown in Fig. 2 for Gusev1 Site1. The BER result for each distance is an average over four different locations at the same distance. Transmitted power is 1 mW for all cases, and 802.11b results are obtained using a RAKE receiver. The data rate for 802.11a is 12 Mbps and the 802.11b transmits at the rate of 11 Mbps. In the case of 802.11a, the overall BER seems to increase with distance except for a strong dip at 500 m. This BER dip is believed to be due to favorable terrain conditions at that distance and it agrees well with the PER result in Table 2. The BER for 802.11b seems to be nearly constant up to distances of 1000 m except for a dip at 500 m similar to 802.11a.

Effect of transmit power on PER

Although Tables 2–6 show PER results for 1 W of transmit power, it is instructive to study the effects of transmit

Table 2. Packet Error Rate Performance at Gusev1 Site1. A ‘-’ indicates zero packet errors, in 20,000 packets.

d (m)	rms delay spread (μ s)		Received power (nW)		PER	
	802.11a	802.11b	802.11a	802.11b	802.11a	802.11b
20	0.194	0.268	40.9	79.3	0.0008	0.0983
50	0.144	0.203	38.6	75	0.0004	0.0768
100	0.105	0.155	36.4	71	0.0001	0.0572
200	0.180	0.153	70.0	206	0.0001	0.0281
500	0.091	0.092	61.7	145	-	0.0158
1000	17.3	1.86	.00011	0.0009	1	0.9619

Table 3. Packet Error Rate performance at Gusev1 Site2.

d (m)	rms delay spread (μ s)		Received power (nW)		PER	
	802.11a	802.11b	802.11a	802.11b	802.11a	802.11b
20	0.146	0.186	38.2	79	0.0003	0.115
50	0.131	0.155	26.7	56	0.0004	0.082
100	0.095	0.126	25.8	54	0.0001	0.032
200	0.713	0.719	0.0822	0.16	0.099	0.51
500	0.472	0.476	0.0114	0.02	0.067	0.53

Table 4. Packet Error Rate performance at Gusev1 Site3. A ‘-’ indicates zero packet errors, in 20,000 packets.

d (m)	rms delay spread (μ s)		Received power (nW)		PER	
	802.11a	802.11b	802.11a	802.11b	802.11a	802.11b
20	0.143	0.17	52.0	119	0.0002	0.1
50	0.055	0.1	45.2	102	-	0.027
100	0.055	0.065	45.9	103	-	0.016
200	0.070	0.089	34.8	81	0.0001	0.03
500	11.2	9.2	.00001	0.0001	1	0.54
1000	0.742	0.718	.000001	.00003	1	1

Table 5. Packet Error Rate Performance at Hematite4 Site1.

d (m)	rms delay spread (μ s)		Received power (nW)		PER	
	802.11a	802.11b	802.11a	802.11b	802.11a	802.11b
20	0.741	0.634	59.2	114.27	0.0262	0.2113
50	0.747	0.625	49.1	94.02	0.0272	0.2844
100	0.584	0.564	47.0	80.62	0.0138	0.1667
200	0.289	0.297	29.3	46.07	0.0026	0.1196
500	0.069	0.087	22.5	43.24	0.0001	0.0478
1000	0.696	0.685	.0374	0.167	0.4405	0.3312

Table 6. Packet Error Rate Performance at Hematite5 Site1.

d (m)	rms delay spread (μ s)		Received power (nW)		PER	
	802.11a	802.11b	802.11a	802.11b	802.11a	802.11b
20	1.031	0.913	45.9	88.54	0.0037	0.1280
50	0.755	0.694	36.2	69.04	0.0012	0.0950
100	0.475	0.498	29.2	55.97	0.0004	0.0724
200	0.178	0.228	28.6	55.30	0.0001	0.0354
500	0.160	0.204	42.3	88.95	0.0004	0.0370
1000	0.287	0.316	$2 \cdot 10^{-7}$	$2 \cdot 10^{-6}$	1	1

Table 7. Effect of Transmit Power on PER for Gusev1 Site1 at a distance of 100 m from the transmitter. The 802.11b receiver is implemented without a RAKE structure.

Transmit Power	PER for 802.11a	PER for 802.11b
1 μ W	0.985	0.4183
10 μ W	0.381	0.1719
100 μ W	0.0225	0.1011
1 mW	0.0021	0.0625
10 mW	4×10^{-4}	0.0612
100 mW	2.5×10^{-4}	0.0555
1 W	2×10^{-4}	0.0516

power on the PER. This is investigated via Table 7 for Gusev1 Site1. The table shows that when the transmit power is small, 802.11b seems to be doing better than 802.11a. As the transmit power increases, the performance for both 802.11a and b tend to flatten out for high transmit power, but 802.11a shows much better performance than 802.11b. Note that the rms delay spread for this location is 0.105μ s for 802.11a, and it is much less than the available 0.8μ s guard period. Thus, 802.11a can handle this delay spread quite well, and its performance keeps improving with the transmit power. As the transmit power becomes large, however, the multipaths with delays exceeding 0.8μ s start affecting its performance with adjacent symbol interference. This limits the performance improvement. In the case of 802.11b too, multipaths do not allow performance improvement beyond a certain value.

BER Performance versus SNR

The bit error rate (BER) performance results versus SNR are shown in Figs. 3-12 for IEEE802.11a and b.

In the case of 802.11a, we notice that lower data rates provide much better BER performance giving several dB advantage over higher rates. However, it is also to be noted that lower rates need to transmit longer than higher rate modes in order to send the same amount of information. We also see that the curves tend to flatten at the higher SNR region as the performance becomes more dominated by the delay spreads. Although the rms delay spread is within 0.8μ s for the cases studied in these figures, there are still multipaths beyond 0.8μ s producing adjacent symbol interference.

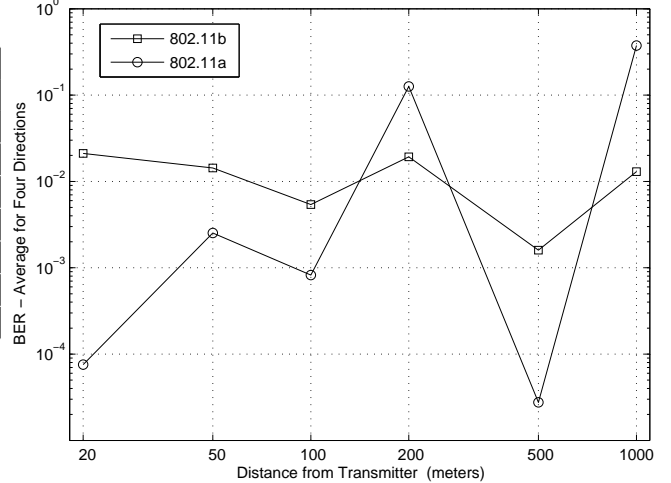


Figure 2. BER Performance for 802.11a and b at Gusev1 Site1.

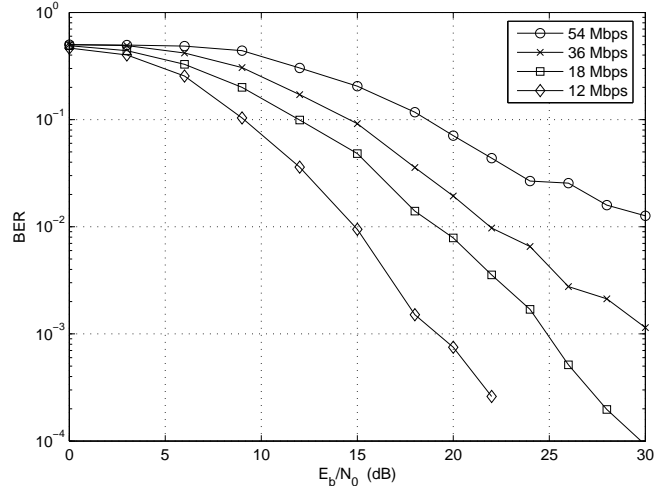


Figure 3. BER Performance for 802.11a at Gusev1 Site1.

The BER performance curves for 802.11b show that multipaths can severely affect their performance. Figures 8-12 show results without a RAKE structure. Another interesting observation is that CCK performs better than the other modulations in some cases.

Effect of using RAKE for 802.11b

The use of a RAKE receiver can significantly improve the BER and PER performance for 802.11b. The BER performance improvements can be seen comparing Figs. 8 and 13 for Gusev1 Site1. The PER performance improvements are summarized in Table 8. The table shows that RAKE can provide PER improvement by a factor as high as eight in this case. The performance improvement seems to be generally smaller at very large distances.

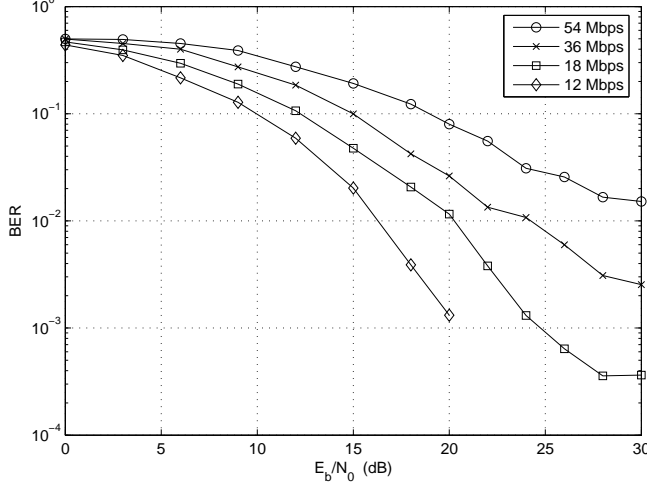


Figure 4. BER Performance for 802.11a at Gusev1 Site2.

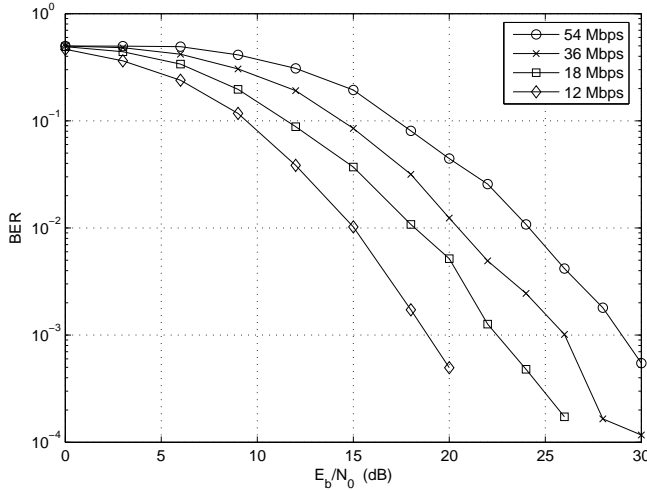


Figure 5. BER Performance for 802.11a at Gusev1 Site3.

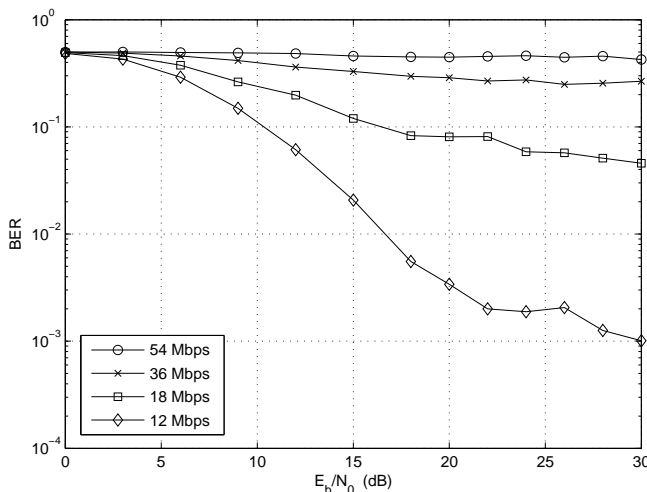


Figure 6. BER Performance for 802.11a at Hematite4 Site1.

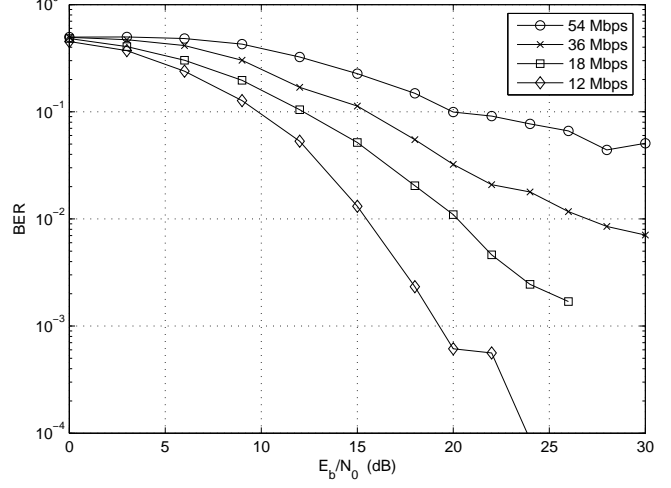


Figure 7. BER Performance for 802.11a at Hematite5 Site1.

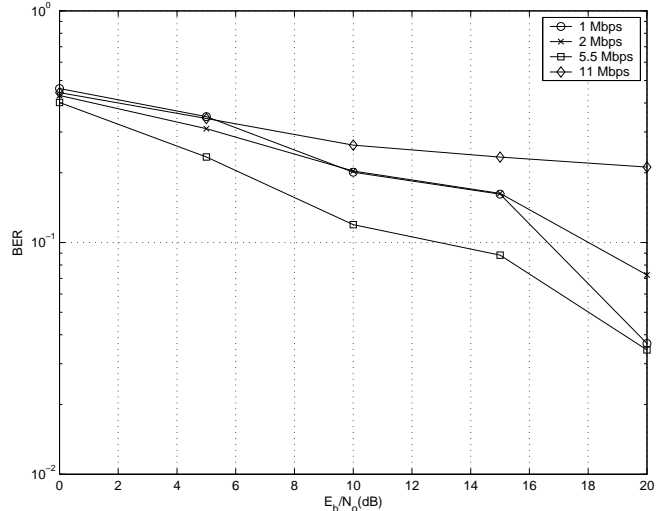


Figure 8. BER Performance for 802.11b at Gusev1 Site1 without a RAKE structure.

Performance versus antenna heights

The antenna heights can affect the performance of both 802.11a and b significantly. An increase in the antenna heights can provide better line-of-sight signals over a rocky terrain and can increase the received power. However, it can result in more delay spreads as well, resulting in decreased performance at the receiver. In the case of 802.11a, we can observe from the PER tables that, of the three sites considered, Gusev1 Site3 has the least rms delay spread at 100 m. Since the received power is too low, the benefit from an increase in the received power becomes significant since the rms delay spread remains much smaller than the guard interval. Thus, when the antenna heights are raised, this site shows significant improvement in performance despite an increase in the rms delay spread value from $0.036 \mu\text{s}$ (corresponding

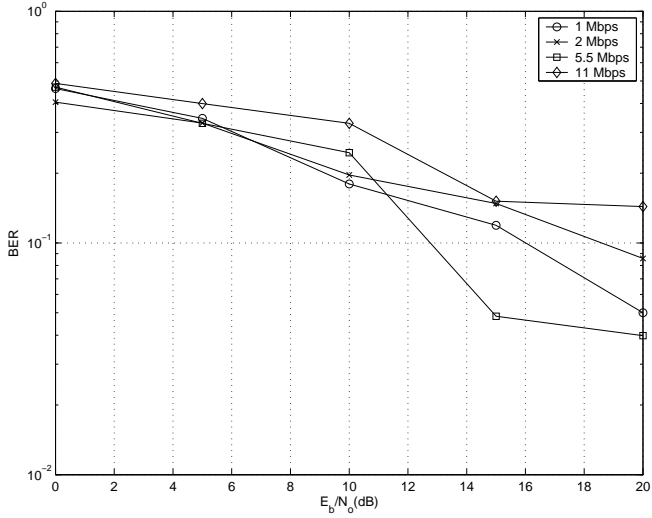


Figure 9. BER Performance for 802.11b at Gusev1 Site2 without a RAKE structure.

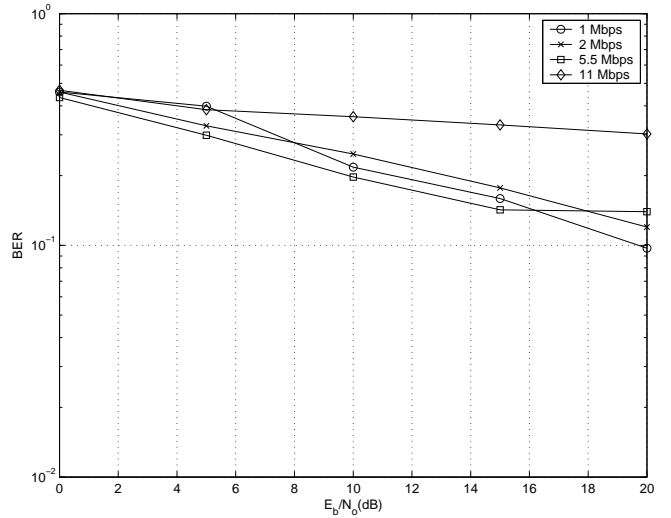


Figure 11. BER Performance for 802.11b at Hematite4 Site1 without a RAKE structure.

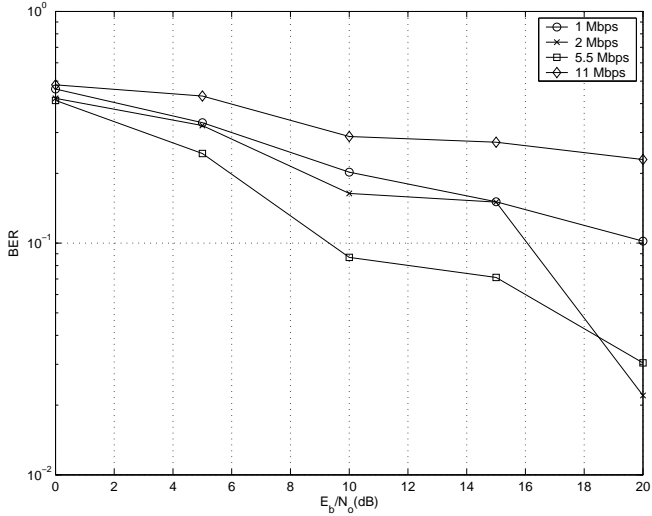


Figure 10. BER Performance for 802.11b at Gusev1 Site3 without a RAKE structure.

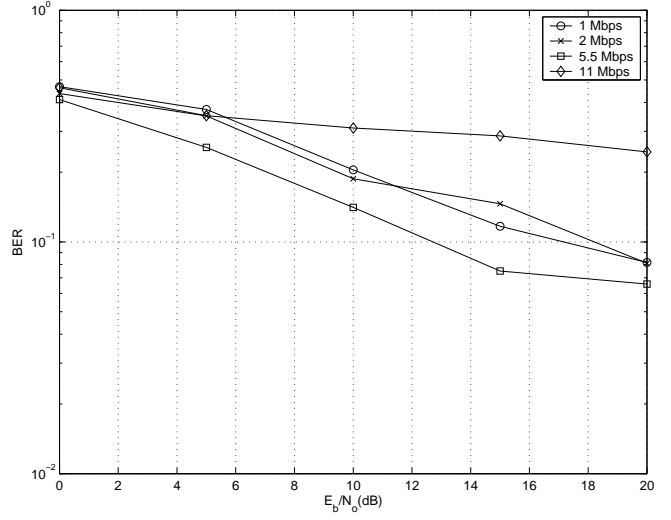


Figure 12. BER Performance for 802.11b at Hematite5 Site1 without a RAKE structure.

to antenna height of 0.5 m) to 0.058 μ s (corresponding to antenna height of 2.0 m). The results in 802.11b do not show significant improvements with antenna heights as in 802.11a. This may be because the benefit due to more received power is nearly cancelled by the loss due to increased delay spreads. Finally, increasing the heights of the antennas beyond a certain value may be impractical for mobile rovers.

5. DISCUSSION

There are several interesting observations.

- The received power for 802.11b is always greater than 802.11a. This makes sense since the transmit frequency for 802.11a is in the 5 GHz band while the transmit frequency for

Table 8. Packet Error Rate Performance at three sites in Gusev1 for IEEE 802.11b. The '-' indicates non-availability of results. The transmit power is 1 W and the antenna heights are fixed at 1.5 m above the ground.

d (m)	Site 1		Site 2		Site 3	
	Without RAKE	With RAKE	Without RAKE	With RAKE	Without RAKE	With RAKE
20	0.098	0.024	0.115	0.022	0.10	0.043
50	0.077	0.014	0.082	0.011	0.027	0.008
100	0.057	0.01	0.032	0.008	0.016	0.005
200	0.028	0.005	0.51	0.284	0.03	0.006
500	0.016	0.002	0.53	0.315	0.54	0.234
1000	0.962	0.52	-	-	1.00	0.682

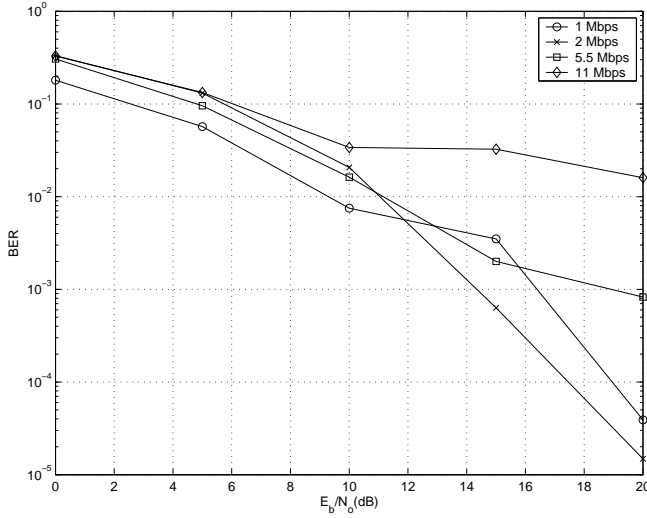


Figure 13. BER Performance for 802.11b at Gusev1 Site1 with a RAKE receiver.

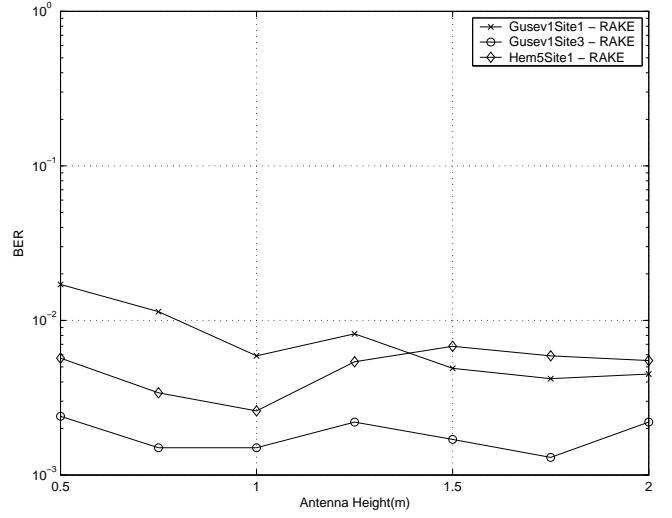


Figure 15. BER Performance for 802.11b at Gusev1 Site1 using a RAKE receiver. The transmit power is $100 \mu\text{W}$, and the distance (d) between the transmitter and the receiver is 100 m.

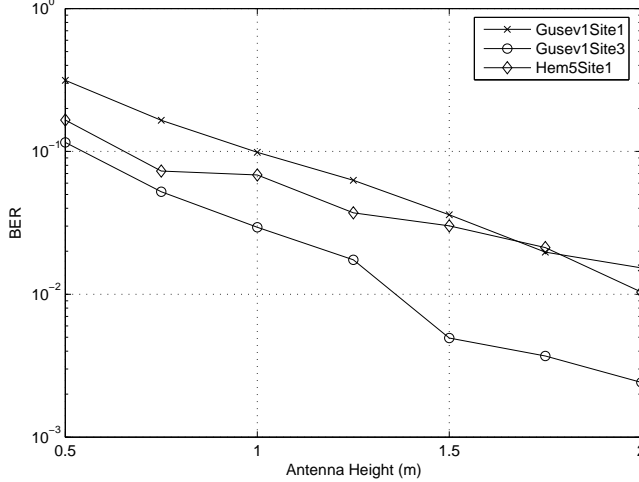


Figure 14. BER Performance for 802.11a at Gusev1 Site1. The transmit power is $100 \mu\text{W}$, and the distance (d) between the transmitter and the receiver is 100 m.

802.11b is in the 2.4 GHz band.

- For shorter distances, the rms delay spread for 802.11a seems to be smaller than for 802.11b in the Gusev sites considered. For larger distances, the rms delay spread for 802.11a increases and becomes similar to or larger than the rms delay spread for 802.11b. The behavior seems to be just the opposite at the Hematite sites.
- The performance of 802.11a and b is affected by received power and multipaths. When the received power is too small, we can say that the system is operating in the power limited region. An increase in power in the power constrained region improves the performance. On the other hand, when sufficient power is received, the performance of the system can still be severely degraded due to multipath effects. In this

case, we can say that the system is in the multipath limited (or equivalently bandwidth limited) region. In the multipath limited region, the performance of the system does not improve with transmission of any additional power.

- The PER for 802.11a is observed to be smaller than the PER for 802.11b in almost all cases for large transmit power (1 W). For smaller transmit power, 802.11b seems to perform better than 802.11a. Note that the received power for 802.11b is larger than for 802.11a as they use 2.4 GHz and 5 GHz frequency bands respectively. This higher received power greatly helps 802.11b in this power limited region. A meaningful comparison between the two, however, should include the effects of packet sizes, overheads, possible improvement due to RAKE in 802.11b, and implementation complexity considerations as well.

6. CONCLUSIONS

In this paper, we have investigated the performance of IEEE 802.11a and b WLAN standards on the Martian surface. We have observed that successful communication is possible within a few hundred meters of the transmit antenna when the transmit power is 1 W and the antenna heights are fixed at 1.5 m above the ground. The packet error rate performance of 802.11b without a RAKE receiver seems to be more adversely affected by the multipaths than 802.11a. Further, the lowest data rate mode of 802.11a provides the best bit error performance. The performance of 802.11b gets improved with the use of a RAKE receiver.

REFERENCES

- [1] “IEEE part 11: Wireless LAN medium access control (MAC) and physical layer (PHY) specifications: High-

speed physical layer in the 2.4 GHz, IEEE Std. 802.11b-1999,” 1999.

- [2] C. Steger, P. Radosavljevic, and J. P. Frantz, “Performance of IEEE 802.11b wireless LAN in an emulated mobile channel,” in *Proc. IEEE VTC*, (Korea), April 2003.
- [3] M. V. Clark, K. K. Leung, B. McNair, and Z. Kostic, “Outdoor IEEE 802.11 cellular networks: Radio link performance,” in *Proc. IEEE ICC*, 2002.
- [4] “IEEE part 11: wireless LAN medium access control (MAC) and physical layer (PHY) specifications: High-speed physical layer in the 5 GHz, IEEE std. 802.11a-1999, sept 1999,” 1999.
- [5] D. K. Borah, R. Jana, and A. Stamoulis, “Performance evaluation of IEEE 802.11a wireless LANs in the presence of ultra-wideband interference,” in *Proc. IEEE Wireless Communications and Networking Conf., WCNC*, (New Orleans), March 2003.
- [6] A. Doufexi, S. Armour, P. Karlsson, A. Nix, and D. Bull, “A comparison of HIPERLAN/2 and IEEE 802.11a,” *IEEE Commun. Magazine*, May 2002.
- [7] V. Chukkala, P. D. Leon, S. Horan, and V. Velusamy, “Modeling the radio frequency environment of mars for future wireless, networked rovers and sensor webs,” in *Proc. IEEE Aerospace Conference*, (Big Sky, MT), 2004.
- [8] “ATDI,” May. 2003. <<http://www.atdi.com>>.
- [9] “NASA Rovers Slated To Examine Two Intriguing Sites On Mars.” NASA News Release 03-137, Apr. 2003. <http://www.nasa.gov/home/hqnews/2003/mar/HP_news_03137.html>.
- [10] A. Rayl, “NASA Announces Mars Exploration Rovers’ Landing Sites,” Apr. 2003. <http://www.planetary.org/html/news/articlearchive/headlines/2003/nasa_mer_sites.htm>.
- [11] C. Ho, S. Slobin, M. Sue, and E. Njoku, “Mars Background Noise Temperatures Received by Spacecraft Antennas,” *The Interplanetary Network Progress Report*, vol. 42-149, May 2002. <http://ipnpr.jpl.nasa.gov/tmo/progress_report/42-149/149C.pdf>.
- [12] P. McKenna. Private communication, Jul. 2003.
- [13] “CommAccess,” Jan. 2004. <<http://www.commaccess.com>>.
- [14] T. H. Lee, H. Samavati, and H. R. Rategh, “5-GHz CMOS Wireless LANs,” *IEEE Trans. on Microwave Theory and Techniques*, vol. 50, pp. 268–279, Jan. 2002.
- [15] D. M. Pozar, *Microwave and RF Wireless Systems*. New York: John Wiley & Sons, 2001.

BIOGRAPHIES



Deva K. Borah received his B.E. and M.E. degrees from the Indian Institute of Science, Bangalore, India, and his Ph.D. degree in telecommunications engineering from the Australian National University, Canberra, Australia in 2000. Since Spring 2000, he has been an Assistant Professor in the Klipsch School of Electrical and Computer Engineering, New Mexico State University, Las Cruces. Dr. Borah serves as a regular reviewer for several major IEEE and IEE journals. His current research interests include detection and estimation techniques, digital communications and digital signal processing.

Mexico State University, Las Cruces. Dr. Borah serves as a regular reviewer for several major IEEE and IEE journals. His current research interests include detection and estimation techniques, digital communications and digital signal processing.



Anirudh Daga received the B.E. degree in Electronics and Telecommunication Engineering from Bombay University, India in 2002. Currently, he is pursuing his M.S. degree in Electrical Engineering at New Mexico State University, Las Cruces. His research interests are in wireless communications.



Gaylon R. Lovelace is a graduate student in Electrical Engineering at New Mexico State University. Prior to NMSU, he worked eleven years in the digital audio and data storage industries. He holds a B.S. in Engineering & Applied Science (1992) from Caltech.



Phillip De Leon received the B.S. Electrical Engineering and the B.A. in Mathematics from the University of Texas at Austin, in 1989 and 1990 respectively and the M.S. and Ph.D. degrees in Electrical Engineering from the University of Colorado at Boulder, in 1992 and 1995 respectively. Previously he worked at AT&T (and later Lucent Technologies) Bell Laboratories in Murray Hill, N.J. Currently, he serves as an Associate Professor in the Klipsch School, Director of the Advanced Speech and Audio Processing Laboratory, and Associate Director of the Center for Space Telemetering and Telecommunications at NMSU. His research interests are in adaptive-, multirate-, real-time-, and speech-signal processing as well as wireless communications. Dr. De Leon is a senior member of IEEE.